

WHIRL FLUTTER ANALYSIS OF A HORIZONTAL-AXIS WIND TURBINE WITH A TWO-BLADED TEETERING ROTOR

David C. Janetzke
NASA Lewis Research Center
Cleveland, Ohio 44135

and

Krishna R. V. Kaza
The University of Toledo
and NASA Lewis Research Center

ABSTRACT

An investigation to explore the possibility of whirl flutter and to find the effect of pitch-flap coupling (δ_3) on teetering motion of the DOE/NASA Mod-2 wind turbine is presented. The equations of motion are derived for an idealized five-degree-of-freedom mathematical model of a horizontal-axis wind turbine with a two-bladed teetering rotor. The model accounts for the out-of-plane bending motion of each blade, the teetering motion of the rotor, and both the pitching and yawing motions of the rotor support. Results show that the Mod-2 design is free from whirl flutter. Selected results are presented indicating the effect of variations in rotor support damping, rotor support stiffness, and δ_3 on pitching, yawing, teetering, and blade bending motions.

INTRODUCTION

Recent horizontal-axis wind turbine (HAWT) designs such as the DOE/NASA Mod-2 wind turbine (ref. 1) include flexible towers in order to achieve significant weight and cost reductions. Experience with prop-rotors has shown that rotors with flexible supports have a potential aeroelastic instability known as whirl flutter. This form of instability involves the interaction of elastic, damping, gyroscopic, and aerodynamic forces. The whirl flutter problem is discussed in references 2-7 among others. In whirl instability, the rotor will precess in a whirl mode with an ever-increasing amplitude when the critical wind speed has been reached. That is, a point on the rotor hub will trace a divergent spiral as illustrated in Figure 1. The direction of the spiral rotation can be either the same as, or counter to, the rotor rotation. These two modes are referred to as forward and backward whirl modes, respectively. Continued operation of a wind turbine in the whirl flutter

mode will quickly lead to failure of the supportive structure. This whirl instability is possible regardless of the presence of rotor teetering motions or blade out-of-plane bending motions. When these motions are included, they couple with the motions of the supportive structure. Then a whirl instability can occur in the whirl modes of the supportive structure and/or the rotor.

Most of the current large HAWT systems have rotors with two blades. The analysis of wind turbines with two-bladed rotors differs significantly from that with axisymmetric rotors. The properties of a two-bladed wind turbine change significantly as the blades rotate from a horizontal to a vertical position. As a result, the equations of motion of a two-bladed wind turbine system contain significant periodic coefficients.

In order to reduce blade bending loads, teetered rotors with pitch-flap coupling (δ_3) have been used in some HAWT systems. The pitch-flap coupling mechanically changes the pitch of the blades as the rotor teeters and thus is equivalent to an aerodynamic spring that restrains teetering motion. The effect of δ_3 on rotor motion stability was studied in refs. 6 and 8. A whirl flutter analysis for a prop-rotor on a flexibly mounted pylon was developed in ref. 6. That analysis may also be suitable for investigation of whirl flutter in HAWT systems. However, since most HAWT systems use rotor blades that are long and relatively flexible, the blade flexibility ought to be included in the formulation of a HAWT whirl flutter analysis.

Other analyses are available for the investigation of whirl flutter in HAWT systems. One is the MOSTAS computer code (refs. 9 and 10). However, it is very complex and uses a large amount of computer time. Hence, it is not well suited to parametric investigations.

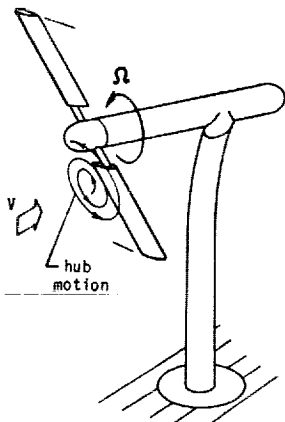


Figure 1. - Wind Turbine Rotor in a Forward Whirl Mode.

Therefore, a simple model, encompassing only the pertinent degrees of freedom, is desired to study the possibility of whirl flutter in a flexibly mounted HAWT.

The primary purpose of this paper is to present the development of a simple model for exploring the possibility of whirl flutter in the DOE/NASA Mod-2 HAWT. Secondary purposes are to study the effects of pitch-flap coupling, rotor support stiffness, and rotor support damping on the response of the Mod-2.

A five-degree-of-freedom mathematical model is developed in the Appendix for a flexibly-mounted two-bladed teetering rotor. The degrees of freedom include the first out-of-plane bending mode for each blade, the rotor teetering motion, the rotor support pitching motion, and the rotor support yawing motion. The developed equations that have periodic coefficients are numerically integrated in the time domain using a standard Runge-Kutta method.

ANALYSIS METHOD

Mathematical Model

The mathematical model of a HAWT with two-bladed teetering rotor is shown in Figure 2. The rotor support is modeled by a rigid pylon of length h that is restrained at one end by two sets of rotational springs and dampers. These springs and dampers represent tower stiffnesses and dampings. The restraints allow only pitching and yawing motions, ϕ_x and ϕ_y , of the pylon. The teetering motion, γ , of the rotor hub with respect to the rotating shaft of the pylon is also restrained by a rotational spring and damper set. The angular velocity, Ω , of the rotor is assumed to be constant. The out-of-plane blade bending deflections are represented by w_1 and w_2 . These deflections are, in turn, expressed in terms of the normal bending modes and the generalized coordinates. Since the blades are relatively stiff, only one mode is considered. This type of representation of the blade motion is referred to as a Rayleigh-type of analysis. As a consequence of this approximation of the blade motion, there are three degrees of freedom for the rotor, one for each blade, and one for

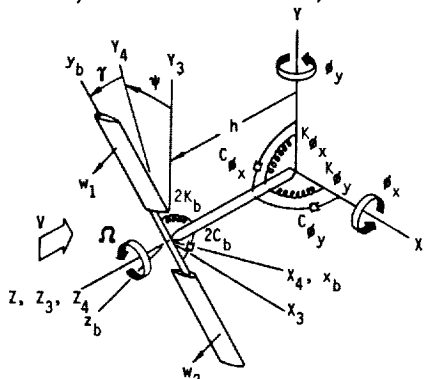


Figure 2. - Mathematical Model of a Two-Bladed Teetering HAWT.

teetering. Thus, with the pitching and yawing motions of the pylon, the wind turbine model has a total of five degrees of freedom. Only the out-of-plane bending motion of the blades is considered because it couples with the rotor teetering motion. Consideration of other motions such as tower translation, blade in-plane bending, and blade torsion are not difficult, but their inclusion would increase the complexity of the analysis. Furthermore, it is believed that these other motions do not have much effect on whirl flutter.

The aerodynamic forces are obtained from strip theory based on a quasi-steady approximation of two-dimensional, incompressible, thin airfoil theory. The blade geometric pitch angle, which consists of the blade built-in twist (pretwist), the pitch angle due to pitch-flap coupling, the collective pitch angle, and the cyclic pitch angle are included in the formulation. Classical blade element momentum theory is used to calculate the steady induced velocity.

Coordinate Systems

Several orthogonal coordinate systems are used in the derivation of the equations of motion. Those that are common to both the dynamic and aerodynamic aspects of the HAWT are described in this section.

1. Inertial system XYZ -- The Y -axis of this system, shown in Figure 2, coincides with the vertical axis of the HAWT tower and is positive upward. The Z -axis coincides with rotor axis and is positive into the wind.
2. Hub system $X_3Y_3Z_3$ -- This system is fixed to the hub center but does not rotate with the rotor. It is parallel to the XYZ system when the pod rotations are zero.
3. Rotor system $X_4Y_4Z_4$ -- This axis system is obtained by rotating the hub system about the Z_3 axis by the rotor position angle ψ ($=\Omega t$) as shown in Figure 2.
4. Blade system $x_b y_b z_b$ -- This axis system is obtained by rotating the rotor system about the X_4 -axis by the rotor teetering angle γ . The y_b axis is aligned along the blade quarter chord points and is also assumed to be the blade elastic axis. The x_b and z_b axes are also shown in Figure 3 along with the various blade element angles, relative velocities, and resultant aerodynamic forces.

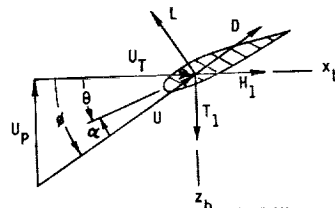


Figure 3. - Blade Element Velocity and Force Vectors for a Wind Turbine Rotor.

Computer Code

The equations of motion developed in the Appendix have timewise periodic coefficients. The stability of a HAWT must be determined by numerically integrating these equations or by using Floquet-Liapunov theory. To this end, a computer program called ASTER5 (Aeroelastic Stability of a Teetering Rotor with 5 degrees of freedom) was written to numerically integrate these equations. The ASTER5 program was first verified by several special cases obtained from ref. 6. The program was then used to investigate the possibility of whirl flutter in the DOE/NASA Mod-2 HAWT and the effect of variations in some of the Mod-2 parameters on its response.

The ASTER5 computer program was written in FORTRAN IV. The input includes the radial distributions of blade chord, twist angle, mass, and first out-of-plane bending mode; equivalent inertia, stiffness, and damping constants for the pylon; and aerodynamic data. The input allows part-span pitchable blades with pitch-flap coupling and cyclic pitch. The program uses a standard subroutine called DVERK, which solves a system of first-order differential equations with a Runge-Kutta method based on Verners fifth- and sixth-order pair of formulas.

RESULTS AND DISCUSSION

To verify the ability of the ASTER5 program to correctly predict whirl flutter, several cases of a prop-rotor, which was analyzed in ref. 6, were evaluated. The parameters for the prop-rotor are presented in Table I. Results are presented for two typical cases. In one case, the prop-rotor response exhibits whirl flutter, while in the other case it is stable. The whirl flutter case in which the pitching and yawing frequencies are 2.3 Hz and 5.0 Hz respectively, is shown in Figure 4. When the pitching frequency is raised to 3.3 Hz by increasing the pitch spring stiffness, the prop-rotor becomes stable, as shown in Figure 5. For comparison, the envelopes of the pitch motion amplitudes for the corresponding cases calculated in ref. 6 are also indicated in Figures 4 and 5. It is evident from

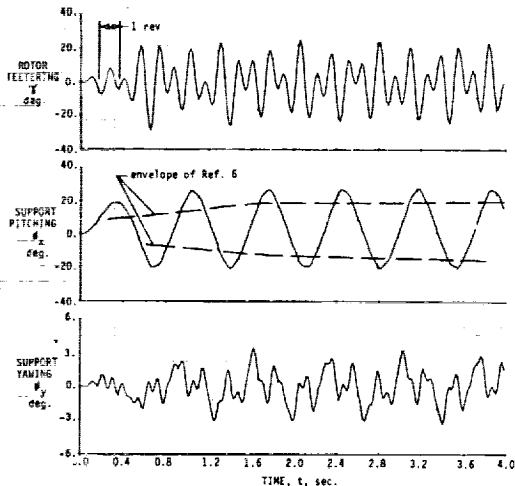


Figure 4. - Response of Prop-Rotor in Whirl Flutter Mode.

these figures that there is agreement between the results of ref. 6 and the ASTER5 program. Thus, the ASTER5 program is capable of predicting whirl flutter. The quantitative differences evident in these figures may be due to differences in airfoil data and/or initial conditions. It should also be noted that ref. 6 does not account for the blade out-of-plane bending motions as does ASTER5. However, the blade frequency is assumed to be high for the input to ASTER5, and thus has a negligible effect on stability. The steady state pitch deflection, ϕ_x , evident in Figure 5, is due to the gravitational moment of the rotor, which is added to the pitching moment only for these verification cases.

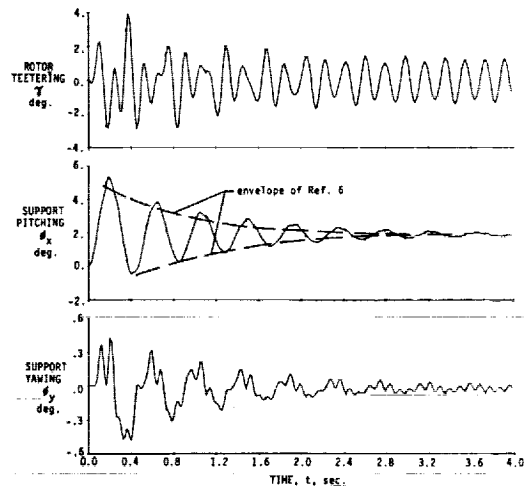


Figure 5. - Response of Prop-Rotor in Stable Mode.

The DOE/NASA Mod-2 HAWT was modeled to investigate the possibility of whirl flutter. The parameters for Mod-2 are presented in Table II. The response of the Mod-2 was calculated with the ASTER5 program. A baseline reference case of the Mod-2 parameters without structural damping was considered for an initial evaluation of its stability. The results of this case, given in Figure 6, show that the pitch, yaw,

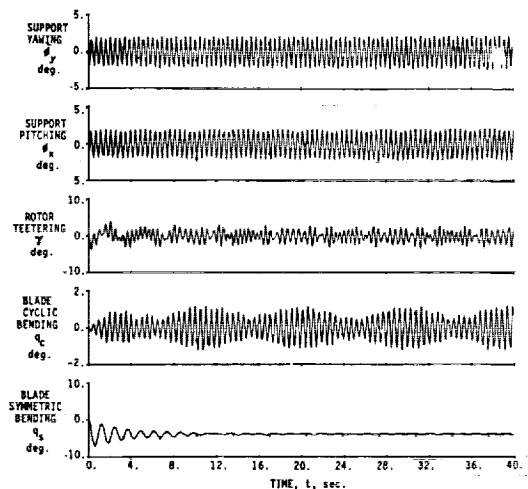


Figure 6. - Response of Mod-2 Baseline Case without Structural Damping.

teeter, and blade cyclic bending motions are neutrally stable. However, when a small amount of structural damping for the pitch and yaw motions is included, all motions are damped out as shown in Figure 7. Since damping exceeding this amount is expected in the actual system, it is concluded that the baseline Mod-2 is free from whirl flutter.

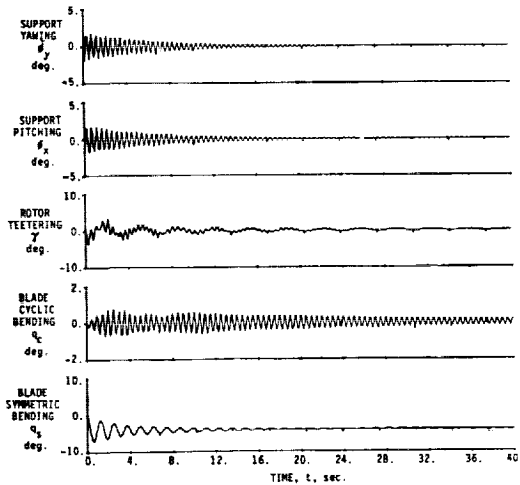


Figure 7. - Response of Mod-2 Baseline Case with Structural Damping ($\zeta\phi_x = \zeta\phi_y = .01$).

To study the effect of pitch-flap coupling on the response of the baseline Mod-2, several cases were calculated for values of δ_3 from -40° to $+40^\circ$. The results indicate that only the blade cyclic bending motion as measured by q_c is affected by variations in δ_3 . Figure 8 shows the change in maximum amplitude of q_c with δ_3 . The results indicate that positive δ_3 has an adverse effect on blade cyclic bending motion.

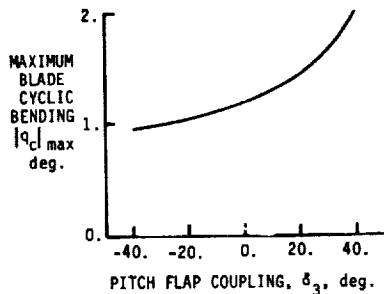


Figure 8. - Effect of Pitch-Flap Coupling, δ_3 , on Blade Cyclic Out-of-Plane Bending Motion.

Other parametric studies were made to explore the possibility of whirl flutter over wide ranges of pylon spring stiffnesses, pylon dampings, rotor rotational speeds, and wind speeds. Some selected results of these studies are presented in Figures 9-12. The possibility of whirl flutter can exist for Mod-2 if the yaw or pitch stiffness of the pylon were substantially reduced. For example, Figure 9 shows the response of Mod-2 when the yaw stiffness is decreased to 6.6% of its baseline value while the other parameters remain the same. These results

indicate whirl flutter by the unstable response of the yaw and teeter motions. When the pylon pitch stiffness is also reduced to 7.3% of its baseline value such that the pitch and yaw frequencies are equal ($\omega\phi_x = \omega\phi_y = 3.665$ Hz), then the response of the pitch motion is also unstable as shown in Figure 10. The whirl motion of the pylon for this case is best illustrated by a cross-plot of the pitch and yaw motion in Figure 11. The figure shows that the system is in a forward whirl mode. From these results, it can be concluded that the stability of a HAWT is highly dependent on the rotor support stiffnesses.

As demonstrated earlier, the stability of a HAWT is sensitive to the presence of structural damping. To further illustrate this fact, a nominal amount of damping ($\zeta\phi_x = \zeta\phi_y = .04$) was added to the unstable case of Figures 10 and 11. The results, shown in Figure 12, indicate that a reasonable amount of structural damping has stabilized all motions of a previously unstable system.

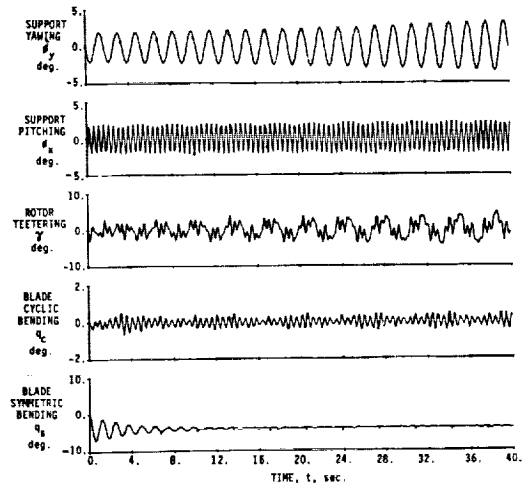


Figure 9. - Response of Mod-2 with Reduced Yaw Stiffness ($\omega\phi_y = 3.665$ Hz).

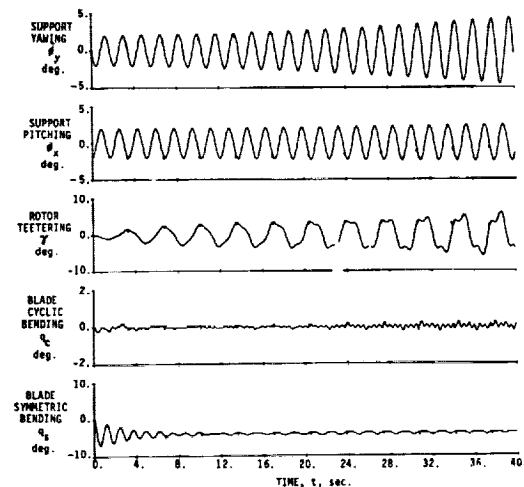


Figure 10. - Response of Mod-2 with Reduced Pitch and Yaw Stiffness ($\omega\phi_x = \omega\phi_y = 3.665$ Hz).

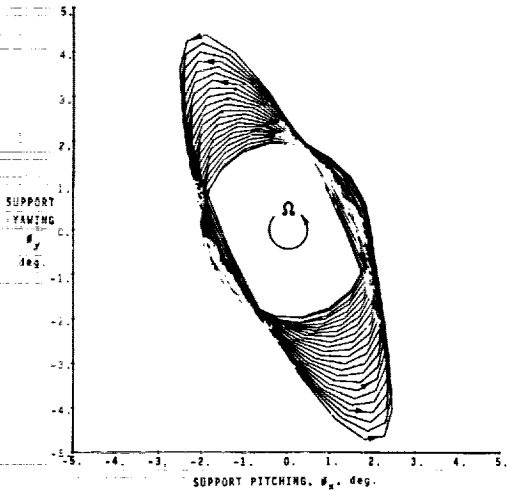


Figure 11. - Hub Motion of Mod-2 with Reduced Pitch and Yaw Stiffness ($\omega_{\phi_x} = \omega_{\phi_y} = 3.665$ Hz) in Whirl Flutter Mode.

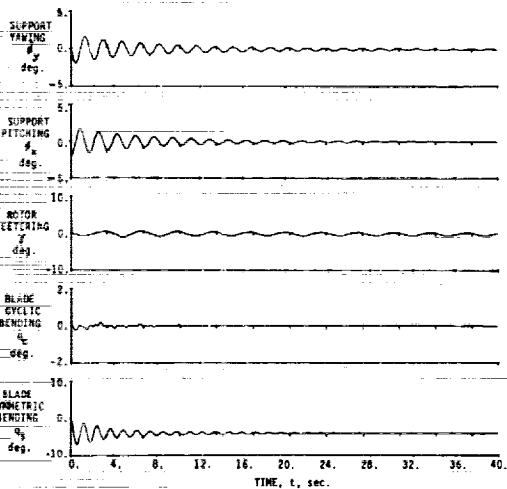


Figure 12. - Response of Mod-2 with Reduced Pitch and Yaw Stiffness ($\omega_{\phi_x} = \omega_{\phi_y} = 3.665$ Hz) and Structural Damping ($\omega_{\phi_x} = \omega_{\phi_y} = .04$).

CONCLUSIONS

An investigation was conducted to explore the possibility of whirl flutter in a large HAWT. A five degree-of-freedom mathematical model and its associated computer program were developed and verified. The program was used to study the possibility of whirl flutter in the DOE/NASA Mod-2 wind turbine and the effect of parametric variations in pitch-flap coupling, rotor support stiffnesses, and structural damping on its response. Based on these limited studies, the following conclusions were obtained.

1. The ASTER5 program is capable of predicting whirl flutter for two-bladed teetering rotor systems.

2. The baseline design of the Mod-2 HAWT is free of whirl flutter.

3. Positive δ_3 has an adverse effect on cyclic blade out-of-plane bending motions for the Mod-2 design, whereas negative δ_3 has little effect.

4. Reduction in rotor support stiffness or structural damping increases the possibility of whirl flutter.

REFERENCES

1. Anon., Mod-2 Wind Turbine System Concept and Preliminary Design Report - Volume II Detailed Report, DOE/NASA 0002-80/2, NASA CR-159609, July 1979.
2. Reed, W. H., Review of Propeller-Rotor Whirl Flutter, NASA TR R-264, July 1967.
3. Kaza, K. R. V., The Effect of Steady State Coning Angle and Damping on Whirl Flutter Stability, J. Aircraft, Vol. 10, November 1973, pp. 664-669.
4. Kvaternik, R. G., Studies in Tilt-Rotor VTOL Aircraft Aeroelasticity, Ph.D. dissertation, Case Western Reserve University, Cleveland, Ohio, June 1973.
5. Johnson, W., Dynamics of Tilting Proprotor Aircraft in Cruise Flight, NASA TN D-7677, May 1974.
6. Hall, W. Earl, Jr., Prop-Rotor Stability at High Advance Ratios, J. Am. Helicopter Society, Vol. 11, No. 2, April 1966, pp. 11-26.
7. Baker, K. E.; Smith, R.; and Toulson, K. W., Notes on Propeller Whirl Flutter, Canadian Aeronautics and Space Journal, Vol. 11, October 1965, pp. 305-313.
8. Gaffey, T. M., The Effect of Positive Pitch-Flap Coupling (Negative γ) on Rotor Blade Motion Stability and Flapping, paper no. 227, Am. Helicopter Society, 24th Annual National Forum Proceedings, Sheraton Park Hotel, Washington, D.C., May 8-10, 1968.
9. Hoffman, J. A., Coupled Dynamic Analysis of Wind Energy Systems, NASA CR-135152, February 1977.
10. Kaza, K. R. V; and Janetzke, D. C., MOSTAS Computer Code Evaluation for Dynamic Analysis of Two-Bladed Wind Turbines, AIAA J. Energy, Vol. 4, No. 4, July-August 1980, pp. 162-169.

NOMENCLATURE

- | | |
|------------------------------------|--|
| c | blade chord length |
| $C_D, C_W, C_{\phi_x}, C_{\phi_y}$ | damping coefficients of rotor teetering, blade out-of-plane bending, pylon pitch and yaw motions, respectively |
| D | profile drag per unit length of blade element |

h	pylon length
H	total rotor shear force, Eq. (A20)
H ₁ , H ₂	rotor shear force per unit length of blade 1 and 2, respectively
I _b	mass moment of inertia of the blade defined in Eq. (A9)
I _{px} , I _{py}	mass moments of inertia of the pylon about the X and Y axes
K _b	half of the teeter spring stiffness
K _c , K _w	effective blade spring stiffnesses defined in Eq. (A11)
K _{φx} , K _{φy}	pylon spring stiffnesses
L	circulatory lift per unit length of blade element
M _b , M _{b2}	mass properties of the blade defined in Eq. (A9)
q _c , q _s	cyclic and symmetric coordinates for blade out-of-plane bending motions defined in Eq. (A9)
q _{w1} , q _{w2}	generalized coordinates for out-of-plane bending motions of blades 1 and 2
r	radial distance along blade elastic axis
R	radial length of blade
S _{b1}	mass property of blade defined in Eq. (A9)
t	time
T	total rotor thrust force, Eq. (A20) also kinetic energy
T ₁ , T ₂	rotor thrust force per unit length of blade 1 and 2
U	resultant aerodynamic velocity, also potential energy
U _p , U _T	components of U, Figure 3
v	induced velocity
V	wind velocity
w ₁ , w ₂	out-of-plane bending deflections of blade 1 and 2
x _b , y _b , z _b	blade coordinate system
X, Y, Z	inertial coordinate system
X ₃ , Y ₃ , Z ₃	hub coordinate system

X ₄ , Y ₄ , Z ₄	rotor coordinate system
α	blade angle of attack
γ	rotor teeter deflection angle
δ ₃	pitch-flap coupling angle Eq. (A22)
ζ _b , ζ _w , ζ _{φx} , ζ _{φy}	critical damping ratios, Eq. (A13)
θ, θ _t , θ ₀ , θ _{1c} , θ _{1s}	blade pitch, twist, collective pitch, and cyclic pitch angles
ρ	air density
φ	aerodynamic inflow angle
φ _x , φ _y	pylon rotational deflections
Φ	normalized blade mode shape
ψ	rotor position angle
ω _b	blade natural frequency
ω _w	blade out-of-plane bending frequency
ω _{φx}	pylon frequency ($=\sqrt{K_{\phi x}/I_{\phi x}}$)
ω _{φy}	pylon frequency ($=\sqrt{K_{\phi y}/I_{\phi y}}$)
Ω	rotor rotational speed
(·)	time derivative
{ }	column matrix
[]	square matrix

TABLE I. PARAMETERS FOR PROP-ROTOR OF REF. 6

Air velocity, V	77.1 m/s
Rotor	
Radial length, R	3.505 m
Rotational speed,	320 RPM
Pitch-flap coupling, δ ₃	20°
Teeter spring stiffness, 2K _b	0
Teeter motion damping, 2ζ _b	0
Blade	
Mass properties	
M _b	26.09 kg
M _{b2}	16.96 kg-m ²
S _{b1}	42.17 kg-m ²
I _b	118.9 kg-m ²
Stiffness, (K _c +K _w)	.3821x10 ⁶ N-m/rad
Damping, ζ _w	0
Airfoil	NACA 0015
Chord, c	.2794 m
Twist distribution, θ _t (r)	
0 < r/R ≤ .45	.677-1.217r/R rad
.45 < r/R ≤ 1.0	.419(.75-r/R) rad
Collective pitch, θ ₀	.74 rad
Pylon Properties	
Inertias, I _{px} = I _{py}	21.60 kg-m ²
Stiffness,	
K _{φx}	29.71x10 ³ N-m/rad
K _{φy}	140.3x10 ³ N-m/rad
Damping, ζ _{φx} = ζ _{φy}	.04
Length, h	1.143 m

TABLE II. PARAMETERS FOR DOE/NASA MOD-2 HAWT

Wind velocity, V	12.2 m/s
Rotor	
Radial length, R	45.81 m
Rotational speed,	17.5 RPM
Pitch-flap coupling, δ_3	0
Teeter spring stiffness, $2K_b$	0
Teeter motion damping, $2\zeta_b$	0
Blade	
Mass properties	
M_b	26021. kg
M_{b2}	.9125x10 ⁶ kg-m ²
S_{b1}	3.368x10 ⁶ kg-m ²
Stiffness, (K_c+K_w)	78.82x10 ⁶ N-m/rad
Damping, ζ_w	0
Airfoil	NACA 23018
Chord distribution, c(r)	
.1542 ≤ r/R ≤ .3455	3.319-8.429(.3455-r/R) m
.3455 < r/R ≤ 1.0	1.436+2.877(1-r/R) m
Twist distribution, $\theta_t(r)$	
.1542 ≤ r/R ≤ .27	.03459-.155(.27-r/R) rad
.27 < r/R ≤ 1.0	-.0698 + .143(1-r/R) rad
Collective pitch, θ_b	
.1542 ≤ r/R < .7006	0
.7006 ≤ r/R ≤ 1.0	-.05236 rad
Pylon	
Inertia,	
I_{px}	6.115x10 ⁶ N-m ²
I_{py}	.6210x10 ⁶ N-m ²
Stiffness,	
K_{ϕ_x}	6.183x10 ⁹ N-m/rad
K_{ϕ_y}	3.140x10 ⁹ N-m/rad
Damping,	
ζ_{ϕ_x}	0
ζ_{ϕ_y}	0
Length, h	7.3152 m

where

$$[T_{\phi_x}] = \begin{bmatrix} 1 & 0 & 0 \\ 0 & \cos \phi_x & -\sin \phi_x \\ 0 & \sin \phi_x & \cos \phi_x \end{bmatrix}$$

$$[T_{\phi_y}] = \begin{bmatrix} \cos \phi_y & 0 & \sin \phi_y \\ 0 & 1 & 0 \\ -\sin \phi_y & 0 & \cos \phi_y \end{bmatrix} \quad (A3)$$

The position vector of a point on blade 1 can be written in the $X_3Y_3Z_3$ axis system as

$$\bar{r}_3 = [T_{\psi}][T_{\gamma}] \begin{Bmatrix} 0 \\ r \\ w_1(r, t) \end{Bmatrix} \quad (A4)$$

where

$$[T_{\psi}] = \begin{bmatrix} \cos \psi & -\sin \psi & 0 \\ \sin \psi & \cos \psi & 0 \\ 0 & 0 & 1 \end{bmatrix}$$

$$[T_{\gamma}] = \begin{bmatrix} 1 & 0 & 0 \\ 0 & \cos \gamma & -\sin \gamma \\ 0 & \sin \gamma & \cos \gamma \end{bmatrix} \quad (A5)$$

Combining Equations (A2) and (A4), the position vector of a point on the axis of blade 1 expressed in the XYZ axis system is

$$\bar{r} = [T_{\phi_x}][T_{\phi_y}] \begin{Bmatrix} 0 \\ 0 \\ h \end{Bmatrix} + [T_{\psi}][T_{\gamma}] \begin{Bmatrix} 0 \\ r \\ w_1(r, t) \end{Bmatrix} \quad (A6)$$

where $w_1(r, t)$ is represented by a single elastic blade mode and is

$$w_1(r, t) = \phi(r)q_{w_1}(t) \quad (A7)$$

The position vector of a point on the axis of blade 2 is obtained from Equations (A6) by replacing w_1 , γ , and ψ by w_2 , $-\gamma$, and $\psi+\pi$ respectively.

APPENDIX

Derivation of Equation of Motion

The mathematical model of a horizontal axis wind turbine is shown in Figure 2. The degrees of freedom and the required coordinate systems are described in the main body of this paper. The equations of motion, herein, have been derived by using the Lagrangian approach. This formulation requires expressions for the position vectors of arbitrary points on the pylon and the blades. These expressions are obtained with the aid of a series of rotations. The order of the rotations, illustrated in Figure 2, is ϕ_x , ϕ_y , ψ , and γ . The position vector of a point on the pylon axis is

$$\bar{r}_p = [T_{\phi_x}][T_{\phi_y}] \begin{Bmatrix} 0 \\ 0 \\ s_p \end{Bmatrix} \quad (A1)$$

and that of the hub-nylon axis junction point is

$$\bar{r}_{ph} = [T_{\phi_x}][T_{\phi_y}] \begin{Bmatrix} 0 \\ 0 \\ h \end{Bmatrix} \quad (A2)$$

The total kinetic energy of the pylon and the rotor is formed from the position vectors given by Equations (A1) and (A6) and is given by

$$\begin{aligned}
 T = & \frac{1}{2} \left\{ [I_{\phi_x} + I_b(1 - \cos 2\psi)] \dot{\phi}_x^2 \right. \\
 & + [I_{\phi_y} + I_b(1 - \cos 2\psi)] \dot{\phi}_y^2 \\
 & + [-4S_{b1}\gamma q_c - 2I_b\gamma^2 + 2I_b]\Omega^2 \\
 & + 2I_b\dot{\gamma}^2 + 2M_{b2}(\dot{q}_s^2 + \dot{q}_c^2) + 2\dot{\phi}_x\dot{\phi}_y I_b \sin 2\psi \\
 & + 4\dot{\phi}_x\Omega [S_{b1}q_c \sin \psi + I_b\gamma \sin \psi] \\
 & + 4\dot{\phi}_x\dot{\gamma} I_b \cos \psi + 4\dot{\phi}_x\dot{q}_c S_{b1} \cos \psi \\
 & - 4\dot{\phi}_y\Omega [I_b\phi_x + S_{b1}q_c \cos \psi + I_b\gamma \cos \psi] \\
 & + 4\dot{\phi}_y\dot{\gamma} I_b \sin \psi + 4\dot{\phi}_y S_{b1}\dot{q}_c \sin \psi \\
 & \left. + 4S_{b1}\dot{\gamma}\dot{q}_c \right\} \quad (A8)
 \end{aligned}$$

where

$$\begin{aligned}
 I_{\phi_x} &= I_{P_x} + 2M_b h^2 \\
 I_{\phi_y} &= I_{P_y} + 2M_b h^2 \\
 M_b &= \int_0^R m_b dr \\
 I_b &= \int_0^R m_b r^2 dr \\
 S_{b1} &= \int_0^R m_b \phi r dr \\
 M_{b2} &= \int_0^R m_b \phi^2 dr \\
 q_s &= (q_{w1} + q_{w2})/2 \\
 q_c &= (q_{w1} - q_{w2})/2
 \end{aligned} \quad (A9)$$

The quantities I_{P_x} and I_{P_y} are the pylon inertias about the X and Y axes, respectively.

The potential energy of the pylon and the rotor can be written as

$$\begin{aligned}
 U = & \frac{1}{2} [K_{\phi_x}\phi_x^2 + K_{\phi_y}\phi_y^2 + 2K_b\gamma^2 \\
 & + 2(K_w + K_c)(q_s^2 + q_c^2)] \quad (A10)
 \end{aligned}$$

where

$$\begin{aligned}
 K_w &= \int_0^R EI_{y_b y_b} \phi''^2(r) dr \\
 K_c &= \int_0^R T_c \phi'^2(r) dr \\
 T_c &= \int_r^R m_b \Omega^2 r dr
 \end{aligned} \quad (A11)$$

The dissipation potential for the pylon and the rotor can be written as

$$\begin{aligned}
 U_D = & \frac{1}{2} [C_{\phi_x}\dot{\phi}_x^2 + C_{\phi_y}\dot{\phi}_y^2 + 2C_b\dot{\gamma}^2 \\
 & + 2C_w(q_s^2 + q_c^2)] \quad (A12)
 \end{aligned}$$

where

$$\begin{aligned}
 C_{\phi_x} &= 2\zeta_{\phi_x} I_{\phi_x} \omega_{\phi_x} \\
 C_{\phi_y} &= 2\zeta_{\phi_y} I_{\phi_y} \omega_{\phi_y} \\
 C_b &= 2\zeta_b I_b \omega_{\gamma} \\
 C_w &= 2\zeta_w M_{b2} \omega_b
 \end{aligned} \quad (A13)$$

By substituting Equations (A8), (A10), and (A12) into Lagrangian equations of the form

$$\frac{d}{dt} \left(\frac{\partial T}{\partial \dot{q}_i} \right) - \frac{\partial T}{\partial q_i} + \frac{\partial U}{\partial q_i} + \frac{\partial U_D}{\partial q_i} = Q_i \quad (A14)$$

the following equations of motion for the wind turbine model are obtained

$$[I]\{\ddot{q}\} + [C]\{\dot{q}\} + [K]\{q\} = \{Q\} \quad (A15)$$

where

$$\{q\} = \begin{Bmatrix} q_s \\ q_c \\ \gamma \\ \phi_x \\ \phi_y \end{Bmatrix} \quad \{Q\} = \begin{Bmatrix} Q_{w1} + Q_{w2} \\ Q_{w1} - Q_{w2} \\ M_{\gamma} \\ M_{\phi_x} \\ M_{\phi_y} \end{Bmatrix}$$

$$[I] = \begin{bmatrix} 2M_{b2} & 0 & 0 & 0 & 0 \\ 0 & 2M_{b2} & 2S_{b1} & 2S_{b1} \cos \psi & 2S_{b1} \sin \psi \\ 0 & 2S_{b1} & 2I_b & 2I_b \cos \psi & 2I_b \sin \psi \\ 0 & 2S_{b1} \cos \psi & 2I_b \cos \psi & I_{\phi_x} + I_b(1 + \cos 2\psi) & I_b \sin 2\psi \\ 0 & 2S_{b1} \sin \psi & 2I_b \sin \psi & I_b \sin 2\psi & I_{\phi_y} + I_b(1 - \cos 2\psi) \end{bmatrix} \quad (A16)$$

$$[C] = \begin{bmatrix} 2C_w & 0 & 0 & 0 & 0 \\ 0 & 2C_w & 0 & -4I_b\Omega \sin \psi & 4S_{b1}\Omega \cos \psi \\ 0 & 0 & 2C_b & -4I_b\Omega \sin \psi & 4I_b\Omega \cos \psi \\ 0 & 0 & 0 & C_{\phi_x} - 2I_b\Omega \sin 2\psi & 2I_b\Omega(1 + \cos 2\psi) \\ 0 & 0 & 0 & -2I_b\Omega(1 - \cos 2\psi) & C_{\phi_y} + 2I_b\Omega \sin 2\psi \end{bmatrix}$$

$$[K] = \begin{bmatrix} 2(K_w + K_c) & 0 & 0 & 0 & 0 \\ 0 & 2(K_w + K_c) & 2S_{b1}\Omega^2 & 0 & 0 \\ 0 & 2S_{b1}\Omega^2 & 2K_b + 2I_b\Omega^2 & 0 & 0 \\ 0 & 2S_{b1}\Omega^2 \cos \psi & 2I_b\Omega^2 \cos \psi & K_{\phi_x} & 0 \\ 0 & 2S_{b1}\Omega^2 \sin \psi & 2I_b\Omega^2 \sin \psi & 0 & K_{\phi_y} \end{bmatrix}$$

The next step is to obtain expressions for Q_{w1} , Q_{w2} , M_γ , M_{ϕ_x} , and M_{ϕ_y} . The expressions are derived from the virtual work of the aerodynamic forces, which can be written as

$$\delta W_A = \sum_{n=1}^2 \int_0^R (\bar{F}_A \cdot \delta \bar{r}) dr \quad (A17)$$

where \bar{F}_A is the aerodynamic force vector per unit length. The components of \bar{F}_A are illustrated in Figure 3 from which one can write

$$\{F_A\}_{\text{blade 1}} = \begin{Bmatrix} H_1 \\ 0 \\ T_1 \end{Bmatrix} \quad (A18)$$

By using a similar expression for blade 2, substituting it with Equations (A6) and (A18) into Equation (A17), and neglecting several higher order terms believed to be unimportant, one obtains

$$\begin{aligned} Q_{w1} &= \int_0^R T_1 \phi \, dr \\ Q_{w2} &= \int_0^R T_2 \phi \, dr \\ M_\gamma &= \int_0^R (T_1 - T_2) r \, dr \end{aligned} \quad (A19)$$

$$M_{\phi_x} = -Hh \sin \psi + Th\gamma \cos \psi + M_\gamma \cos \psi$$

$$M_{\phi_y} = Hh \cos \psi + Th\gamma \sin \psi + M_\gamma \sin \psi$$

where

$$\begin{aligned} H &= \int_0^R (H_1 - H_2) dr \\ T &= \int_0^R (T_1 + T_2) dr \end{aligned} \quad (A20)$$

The expressions for circulatory lift and profile drag per unit length can be written as

$$L = \frac{1}{2} \rho U^2 c_{cL}(\alpha) \quad (A21)$$

$$D = \frac{1}{2} \rho U^2 c_{cD}(\alpha)$$

where, from Figure 3 and Equation (A6), the following expressions are obtained

$$U = \sqrt{U_P^2 + U_T^2}$$

$$\begin{aligned} U_P &= V \cos \phi_x \cos \phi_y \cos \gamma + r \dot{\phi}_x \cos \psi \\ &\quad + r \dot{\phi}_y \sin \psi + r \dot{\gamma} + \dot{q}_{w1} \phi + v \end{aligned}$$

$$\begin{aligned} U_T &= V \cos \phi_x \sin \phi_y \cos \psi - V \sin \phi_x \sin \psi \\ &\quad + h \dot{\phi}_x \sin \psi - h \dot{\phi}_y \cos \psi + r \Omega \cos \gamma \end{aligned} \quad (A22)$$

$$\alpha = \phi - \theta$$

$$\phi = \tan^{-1} \left(\frac{U_P}{U_T} \right)$$

$$\begin{aligned} \theta &= \theta_0 + \theta_t(r) - \gamma \tan \delta_3 \\ &\quad + \theta_{1c} \cos \psi + \theta_{1s} \sin \psi \end{aligned}$$

In the derivation of above expressions for U_P and U_T , several higher order terms, believed to be unimportant, are neglected. Also, circulatory lift, produced by the angular velocity of the local blade section about the y_0 -axis due to blade out-of-plane bending and rotor teetering, is neglected in the expression of Equation (A21). The values of C_L and C_D are nonlinear functions of α and are calculated from airfoil data.

By resolving L and D in Figure 3, the expressions for T_1 and H_1 are

$$\begin{aligned} T_1 &= -L \cos \phi - D \sin \phi \\ H_1 &= -L \sin \phi + D \cos \phi \end{aligned} \quad (A23)$$

The expressions for T_2 and H_2 are the same but the values of L , D , and α are obtained by replacing γ , ψ , and Q_{w1} by $-\gamma$, $\psi + \pi$, and Q_{w2} , respectively in the expressions of Equation (A22).

The induced velocity v in Equation (A22) is based on classical momentum theory and is

$$v = \frac{-V + \sqrt{V^2 + 2T/\rho\pi R^2}}{2} \quad (A24)$$

QUESTIONS AND ANSWERS

D.C. Janetzke

From: A. Wright

Q: What type of failures would result from severe whirl flutter?

A: *Fatigue failure or ultimate limit load failure.*

From: Bill Wentz

Q: How do you increase structural damping in design?

A: *I don't know.*

From: J.A. Kentfield

Q: What magnitude of structural damping can be expected in the pylon of MOD-2 or similar machines?

A: *The damping applied to the pylon in the model represents the equivalent damping of the entire rotor support system which includes the pod and the tower. The Mod-2 welded tower damping is about 2% of critical damping.*

From: Mr. Doman

Q: What influence has the absence of tower bending modes on results?

A: *The tower bending modes are represented by the pylon support stiffness.*

From: P. Anderson

Q: What time step size was used in the integration process? Have any sensitivity tests been carried out to optimize step size?

- A:
1. *An initial time step equal to 36 steps per rotor revolution was arbitrarily chosen. The integration process could change the step size within the initial size as needed for convergence.*
 2. *Several other step sizes were used, but no attempt was made to optimize the size.*